V European Conference on Computational Fluid Dynamics
ECCOMAS CFD 2010
J. C. F. Pereira and A. Sequeira (Eds)
Lisbon, Portugal,14-17 June 2010

COMPARISON OF INTRUSIVE AND NON - INTRUSIVE POLYNOMIAL CHAOS METHODS FOR CFD APPLICATIONS IN AERONAUTICS

G. Onorato[†], G.J.A. Loeven[*], G. Ghorbaniasl[†], H.Bijl[*], C. Lacor[†]

[†]Vrije Universiteit Brussel, Fluid Dynamics and Thermodynamics Research Group
Pleinlaan 2, 1050 Brussel
e-mail: giuseppe.onorato@vub.ac.be

[*]TU Delft, Faculty of Aerospace Engineering
P.O. Box 5058, 2600 GB Delft, The Netherlands
e-mail: g.j.a.loeven@tudelft.nl

Key words: Fluid Dynamics, Polynomial chaos, IPCM, NIPCM, Non - deterministic computations, RAE2822

Abstract. *The strive in aeronautical industry for more robust designs, requires CFD simulations that also account for uncertainties inherently present in e.g. flow conditions or geometries. In a recent EC project (NODESIM - CFD) different methodologies to deal with such so - called non - deterministic flows have been considered. The polynomial chaos (PC) approach, originally developed by Wiener* [5]*, is a very promising approach. It is based on a polynomial decomposition of the uncertain variables, where the uncertainty is lumped in the polynomials and the unknown coefficients of the decomposition become deterministic. Whereas PC is already well established in structural mechanics, its use in CFD is quite recent. The original PC method is an intrusive approach in the sense that it requires extensive modifications in existing, deterministic CFD codes. Within NODESIM - CFD an intrusive approach was developed for compressible Navier - Stokes simulations* [1,2]*. Alternatively non - intrusive approaches have been developed where standard CFD codes can be used. They all require sampling but different approaches exist. In the present context a probabilistic collocation approach is used* [3,4]*. In the present paper the intrusive polynomial chaos method (IPCM) will be compared to the non - intrusive probabilistic collocation methodology (NIPCM) for a 2D turbulent Navier - Stokes flow. The test case is an RAE2822 airfoil at* $M = 0.729$*, angle of attack* $(AOA) = 2.79^\circ$ *and a Reynolds number* $Re = 6.5 \times 10^6$*. Uncertainties are imposed on the inlet Mach number and AOA.*

1 INTRODUCTION

Nowadays Computational Fluid Dynamics (CFD) has become an indispensable tool in the design and development in many key sectors of economic life. Aiming at shorter turnaround times from concept to market, new designs and prototypes are more and more based on computer simulations. In a good design it is essential that the performance of the product is only weakly sensible to varying conditions; e.g. the efficiency of a compressor is only weakly affected by variations in inlet and outlet conditions or variations of the tip clearance or the geometry. The only way to come to such so - called robust designs, is by using non - deterministic CFD where the possible varying conditions are accounted for directly in the simulation. Several methods exist to deal with these uncertainties. In the present paper two non - deterministic approaches for CFD computation are used, based on intrusive and non - intrusive polynomial chaos methods.

2 NON - DETERMINISTIC POLYNOMIAL CHAOS METHODS

Polynomial Chaos Methods (PCMs) represent one class of non - deterministic methods which gained wide acceptance in the CFD community for propagation of the uncertainties in numerical simulations, where the random quantities are subjected to a spectral representation via a Polynomial Chaos expansion [7]. PCMs show interesting advantages with respect to other non - deterministic methods. With respect to the perturbation methods, PCMs can handle more general types of uncertainties while they seem to be more computationally efficient as the basic Monte Carlo methods.

2.1 IPCM

The classical PC method is an intrusive methodology in the sense that the governing equations are altered. This implies that, in order to use the PC methodology, the CFD codes have to be modified. In some cases this can be a disadvantage e.g. for well validated industrial CFD codes, where any extension has a risk of introducing errors but it can deal with a sensible performance increment if used to compute with multiple uncertainties. The Intrusive Polynomial Chaos Method is formulated in a probabilistic framework. The main idea of the IPC methodology is the following. For every uncertainty in the formulation of the mathematical model a new dimension is introduced and the solution is considered dependent on these dimensions. A convergent expansion along these new dimensions is sought in terms of orthogonal basis functions, whose coefficients are used to quantify the uncertainty of the solution. The weighting function of the scalar products of the polynomials corresponds to the PDF of the uncertain input parameters, which ensures the exponential convergence of the stochastic solution. A Galerkin projection of the deterministic equations on the PC space is used to derive equations determining the coefficients of the PC decomposition of the solution.
Suppose $\xi_k(\theta)_{k=1}^{\infty}$ is a set of independent stochastic variables with a known distribution that determines the stochastic input of the problem. Then the solution to the non -

deterministic problem is sought in the form of the following expansion:

$$u(\underline{x},\theta) = a_0\Gamma_0 + \sum_{i_1=1}^{\infty} a_{i_1}(\underline{x})\Gamma_1(\xi_{i_1}(\theta)) + \tag{1}$$

$$\sum_{i_1=1}^{\infty}\sum_{i_2=1}^{i_1} a_{i_1 i_2}(\underline{x})\Gamma_2(\xi_{i_1}(\theta),\xi_{i_2}(\theta)) +$$

$$\sum_{i_1=1}^{\infty}\sum_{i_2=1}^{i_1}\sum_{i_2=1}^{i_2} a_{i_1 i_2 i_3}(\underline{x})\Gamma_3(\xi_{i_1}(\theta),\xi_{i_2}(\theta),\xi_{i_3}(\theta)) + ...$$

where $\Gamma_p(\xi_1(\theta),\xi_2(\theta),...\xi_n(\theta))$ is the Polynomial Chaos of order p. For computational purposes, the generic PC representation (1) must be truncated. This is typically performed by retaining in Eq. 1 all polynomials of order $\leq p$. If a stochastic field is used as input, its Karhunen - Loeve expansion must be truncated in order to end up with a finite set of independent stochastic variables $\xi_k(\theta)_{k=1}^n$. It is also convenient to introduce a one - to - one mapping between the set of indices appearing in the truncated sum corresponding to Eq. 1 and a set of ordered indices, and re - write the truncated sum in a single index form:

$$u(\underline{x},\theta) = \sum_{j=0}^{P} u_j(\underline{x})\Psi_j \tag{2}$$

where Ψ_j denotes the polynomials in single index notation. The total number of polynomials is $P+1$. The relation between P, the PC order p and the dimension n (number of independent variables ξ_k) is given by the following formula:

$$P + 1 = \frac{(p+n)!}{p!n!} \tag{3}$$

All the polynomials in the above expansion are mutually orthogonal, i.e.

$$< \Psi_i\Psi_j > = < \Psi_i^2 > \delta_{ij} \tag{4}$$

with $<>$ denoting inner product

$$< \Psi_i\Psi_j > \equiv \int W(\xi)\Psi_i(\xi)\Psi_j(\xi)d\xi \tag{5}$$

where $\xi = (\xi_1,\xi_2,...,\xi_n)$ and $W(\xi)$ is the weighting function. For the optimal convergence of the PC expansion the weighting function W must be the same as the PDF of random variables ξ_k. The Askey scheme [6] gives the optimal polynomials Ψ_i for different PDFs.

In order to determine the stochastic behavior of the solution process $u(\underline{x},\theta)$, one must determine the deterministic coefficients u_j in Eq. 2. In the full Polynomial Chaos method

this is achieved through the Galerkin approach. Because polynomials Ψ_j are mutually orthogonal, the coefficients u_j satisfy the following relation:

$$u_j = \frac{\langle \Psi_j u \rangle}{\langle \Psi_j^2 \rangle} \tag{6}$$

Consider a stochastic process described by the following PDE cast in a generic form:

$$L(u(\xi), \xi) = 0 \tag{7}$$

where $\xi = (\xi_1(\theta), \xi_2(\theta), ...\xi_n(\theta))$. The resulting equations for u_j are obtained by introducing Eq. 2 into Eq. 7 and taking Galerkin projections onto the truncated basis. This gives P PDEs for determining the coefficients u_j:

$$\left\langle L\left(\sum_{j=0}^{P} u_j(\underline{x})\Psi_j, \xi\right), \Psi_j \right\rangle = 0, \qquad j = 0, ...P \tag{8}$$

For instance consider the x component of the momentum equation of the 1D compressible Navier - Stokes equation:

$$\frac{\partial \rho u}{\partial t} + \frac{\partial \rho u^2}{\partial x} = -\frac{\partial \Pi}{\partial x} + \frac{\partial \tau_{xx}}{\partial x} \tag{9}$$

where Π is pressure. Using the following expansions:

$$u(x,t,\theta) = \sum_{j=0}^{P} u_j(x,t)\Psi_j \tag{10}$$

$$\Pi(x,t,\theta) = \sum_{j=0}^{P} \Pi_j(x,t)\Psi_j \tag{11}$$

$$\rho(x,t,\theta) = \sum_{j=0}^{P} \rho_j(x,t)\Psi_j \tag{12}$$

the procedure described above leads to

$$\sum_{i=0}^{P}\sum_{j=0}^{P} M_{ijl}\frac{\partial \rho_i u_j}{\partial t} + \sum_{i=0}^{P}\sum_{j=0}^{P}\sum_{k=0}^{P} L_{ijkl}\frac{\partial \rho_i u_j u_k}{\partial x} = -\frac{\partial \Pi_l}{\partial x} + \frac{\partial \left(\tau_{xx}\right)_l}{\partial x}, \quad l = 0, ..., P \tag{13}$$

with

$$M_{ijl} = \frac{\langle \Psi_i \Psi_j \Psi_l \rangle}{\langle \Psi_l^2 \rangle} \tag{14}$$

$$L_{ijkl} = \frac{\langle \Psi_i \Psi_j \Psi_k \Psi_l \rangle}{\langle \Psi_l^2 \rangle} \tag{15}$$

Formally the operational count of these sums are of $O(P^3)$ and $O(P^4)$, respectively. However, due to the sparse nature of both tensors, the operation count is actually much smaller. Still, the evaluation of the Galerkin projections of cubic term is very costly. One can reduce the computational costs by applying the a pseudo - spectral approach. First, the Galerkin projection of the momentum is evaluated as

$$(\rho u)_k = \sum_{i=0}^{P} \sum_{j=0}^{P} M_{ijk} \rho_i u_j \tag{16}$$

Then the Galerkin projections of the cubic term are calculated as:

$$(\rho u^2)_k = \sum_{i=0}^{P} \sum_{j=0}^{P} M_{ijk} (\rho u)_i u_j \tag{17}$$

This approach leads to a significant reduction in computation costs.

2.2 NIPCM

The non - intrusive Probabilistic Collocation method (NIPCM) starts with a polynomial chaos expansion based on Lagrange polynomials. To compute the Galerkin projection and to integrate the approximation to find the mean and variance, Gauss quadrature is used. The use of Gauss quadrature results in a decoupled set of equations, which makes the method non - intrusive. The choice of the weighting function for the Gauss quadrature rule is very important. To assure spectral convergence, the weighting function has to be equal to the probability density function on the uncertain input parameter.

Probabilistic Collocation expansion

The solution and each variable depending on the uncertain input parameter is expanded as follows:

$$u(\mathbf{x}, t, \omega) = \sum_{i=1}^{N_p} u_i(\mathbf{x}, t) h_i\left(\xi(\omega)\right) \tag{18}$$

where the solution $u(\mathbf{x}, t, \omega)$ is a function of space $\mathbf{x}$ and time t and the random event $\omega \in \Omega$, and the number of collocation points N_p. The complete probability space is given by $(\Omega, \mathcal{F}, P)$, with Ω the set of outcomes, $\mathcal{F} \subset 2^\Omega$ the σ-algebra of events and $P : \mathcal{F} \to [0, 1]$ a probability measure. Furthermore, $u_i(\mathbf{x}, t)$ is the solution $u(\mathbf{x}, t, \omega)$ at the collocation point ω_i; h_i is the Lagrange interpolating polynomial chaos corresponding to the collocation point ω_i; ξ is the random basis. The Lagrange interpolating polynomial is a function in terms of the random variable $\xi(\omega)$, which is chosen such that the uncertain

input parameter is a linear transformation of $\xi(\omega)$. The Lagrange interpolating polynomial chaos is the polynomial chaos $h_i\left(\xi(\omega)\right)$ that passes through the N_p collocation points, with $h_i\left(\xi(\omega_j)\right) = \delta_{ij}$. When multiple uncertain parameters are present, the collocation points are obtained from tensor products of one dimensional points. The number of collocation points N_p then becomes $N_p = (P+1)^d$, where P is the order of approximation and d then dimension of the stochastic problem (i.e. number of uncertain parameters). To find the suitable Gauss quadrature points and weights the procedure below is followed.

Computing Gaussian quadrature points with corresponding weights

A powerful method to compute Gaussian quadrature rules is by means of the Golub - Welsch algorithm [8]. This algorithm requires the recurrence coefficients [9] of polynomials which are orthogonal with respect to the weighting function of the integration. Spectral convergence for arbitrary probability distributions is obtained when the polynomials are orthogonal with respect to the probability density function of ξ, so $w(\xi) = f_\xi(\xi)$ [4]. The required recurrence coefficients are computed using the discretized Stieltjes procedure [10], which is a stable method for arbitrary distribution functions.

Orthogonal polynomials satisfy the following three - term recurrence relation:

$$\begin{aligned} \Psi_{i+1}(\xi) &= (\xi - \alpha_i)\Psi_i(\xi) - \beta_i\Psi_{i-1} \qquad\qquad i = 1, 2, \ldots, N_p \\ \Psi_0(\xi) &= 0, \;\; \Psi_1(\xi) = 1 \end{aligned} \tag{19}$$

where α_i and β_i are the recurrence coefficients determined by the weighting function $w(\xi)$ and $\{\Psi_i(\xi)\}_{i=1}^{N_p}$ is a set of (monic) orthogonal polynomials with $\Psi_i(\xi) = \xi^i + \mathcal{O}(\xi^{i-1}), i = 1, 2, \ldots, N_p$. The recurrence coefficients are given by the Darboux's formulae [9]:

$$\begin{aligned} \alpha_i &= \frac{(\xi\Psi_i, \Psi_i)}{(\Psi_i, \Psi_i)} \qquad\qquad i = 1, 2, \ldots, N_p \\ \beta_i &= \frac{(\Psi_i, \Psi_i)}{(\Psi_{i-1}, \Psi_{i-1})} \qquad\qquad i = 2, 3, \ldots, N_p \end{aligned} \tag{20}$$

where $(\cdot, \cdot)$ denotes an inner product. The first coefficient β_1 is given by (Ψ_1, Ψ_1). Gander and Karp [10] showed that discretizing the weighting function leads to a stable algorithm. Stieltjes' procedure starts with $i = 1$. With Eq. 20 the first coefficient α_1 is computed, $\beta_1 = \sum_{j=1}^{N} w_j$. Now $\Psi_2(\xi)$ is computed by Eq. 19 using α_1 and β_1. This is repeated for $i = 2, 3, \ldots, N_p$. When continuous weighting functions are considered $N_p \ll N$, for discrete measures $N_p \leq N$. The inner product is defined as

$$(p(\xi), q(\xi)) = \int_S p(\xi)q(\xi)w_N(\xi)\mathrm{d}\xi = \sum_{j=1}^{N} w_j p(\xi_j)q(\xi_j) \tag{21}$$

for two functions $p(\xi)$ and $q(\xi)$.

From the recurrence coefficients α_i and β_i, $i = 1, 2, \ldots, N_p$, the collocation points ξ_i and corresponding weights w_i are computed using the Golub - Welsch algorithm [8]. With the recurrence coefficients the following matrix is constructed:

$$J = \begin{bmatrix} \alpha_1 & \sqrt{\beta_2} & & & & \\ \sqrt{\beta_2} & \alpha_2 & \sqrt{\beta_3} & & \emptyset & \\ & \sqrt{\beta_3} & \alpha_3 & \sqrt{\beta_4} & & \\ & & \ddots & \ddots & \ddots & \\ & \emptyset & & \sqrt{\beta_{N_p-1}} & \alpha_{N_p-1} & \sqrt{\beta_{N_p}} \\ & & & & \sqrt{\beta_{N_p}} & \alpha_{N_p} \end{bmatrix} \tag{22}$$

The eigenvalues of J are the collocation points ξ_i, $i = 1, \ldots, N_p$, which are the roots of the polynomial of order N_p from the set of the constructed orthogonal polynomials. The distribution of ξ is used to map the collocation points to the input parameters. The weights are found by $w_i = \beta_1 v_{1,i}^2$, $i = 1, \ldots, N_p$, where $v_{1,i}$ is the first component of the normalized eigenvector corresponding to eigenvalue ξ_i.

From the distribution one can extract the probability density function or confidence intervals. The mean and variance of the solution are found by

$$\mu_u = \sum_{i=1}^{N_\mathrm{p}} u_i(\mathbf{x}, t) w_i, \tag{23}$$

$$\sigma_u^2 = \sum_{i=1}^{N_\mathrm{p}} \left(u_i(\mathbf{x}, t)\right)^2 w_i - \left(\sum_{i=1}^{N_\mathrm{p}} u_i(\mathbf{x}, t) w_i \right)^2 \tag{24}$$

where w_i are the weights corresponding to the collocation points ω_i. These relations are derived from the definition of the mean and variance.
A stochastic computation is now performed as follows:

1. *Specify input distributions* for every uncertain parameter by determining the probability density function.

2. *Compute collocation points and weights* based on the probability density functions of the uncertain parameter, using Eq. 20 and Eq. 22.

3. *Perform deterministic computations* for every collocation point. These computations can be performed in parallel.

4. *Construct the stochastic solution* using all obtained deterministic solutions, e.g. mean / variance fields, uncertainty bars or probability density functions, using Eqs. 18, 23 and 24.

3 IPCM AND NIPCM COMPARISON: RAE2822

The proposed application involves the computation of the flow around a transonic RAE2822 airfoil. The free stream flow conditions are $Re = 6.5 \times 10^6$, $M = 0.729$ and angle of attack $\alpha = 2.79°$.

Two cases are considered: one taking into account the uncertainty on the inlet Mach number with a standard deviation of 0.005 and another one considering the uncertainty on the AOA with a standard deviation of 0.1°. For both cases the results of IPCM and NIPCM will be compared. The uncertainties have a normal distribution implying the use of Hermite polynomials according to the Askey scheme [6].

The flow solver used was FINE^{TM}/ Turbo of Numeca Int.; in addition FINE^{TM}/ Hexa has also been used for NIPCM . The structured mesh used in the FINE^{TM}/ Turbo simulations contains 17028 cells, whereas in the FINE^{TM}/ Hexa simulations an unstructured grid of 76063 cells was used, Fig. 1. In all calculations the Spalart - Allmaras turbulence model was used.

In Fig. 2 the FINE^{TM}/ Turbo solution of the averaged pressure coefficient along the surface is compared for IPCM and NIPCM for uncertain AOA and uncertain Mach number. 3^{rd} order PC is used and results are compared with experimental data [11] as well as with the deterministic solution. For the AOA uncertainty a good matching with experimental results is obtained for both IPCM and NIPCM. Note that, near the shock position, the NIPCM results differ somewhat from the deterministic and the IPCM solution. For the Mach number uncertainty, the IPCM solution looks similar to the deterministic solution, whereas the difference with NIPCM is more pronounced than for uncertainty on AOA, with also a deviation at the leading edge on the suction side.

Fig. 3 shows the standard deviation of C_P along the airfoil surface. These plots also contain NIPCM results obtained with FINE^{TM}/ Hexa on a much finer mesh. It can be observed that for AOA uncertainty, Fig. 3(a), in contrast to the IPCM results, no variance peak near the shock position is found with NIPCM. The NIPCM results of FINE^{TM}/ Hexa (on the finer mesh) predict again such a peak, though much smaller than the one of IPCM. Also note that the predicted shock position with FINE^{TM}/ Hexa is different from that of FINE^{TM}/ Turbo which is probably due to the finer mesh. It can also be observed that, apart from the peak, the NIPCM results with Hexa and Turbo are very similar and are systematically higher than the IPCM results, especially on the suction side.

For Mach number uncertainty, Fig. 3(b), all the simulations predict a variance peak near the shock. For the IPCM and NIPCM results obtained with Turbo, the magnitude of the peak near the shock is more or less the same, whereas the NIPCM results of Hexa predict

a higher peak, again shifted upward due to different shock position.

Fig. 4 shows the variance on the Mach number in the flow domain near the airfoil for AOA uncertainty for IPCM and NIPCM with Turbo. In both cases there is an increase of variance near the shock, but in case of NIPCM this increase does not extend to the airfoil. The shape of the Mach number standard deviation looks similar for both computations, but the magnitude is generally higher for IPCM. A layer of increased variance can also be observed near the airfoil downstream of the impingement of the shock.

In case of Mach number uncertainty, Fig. 5, the IPCM and NIPCM results are quite similar everywhere and also the magnitude is comparable. Note again the layer of increased variance near the airfoil after shock impingement.

Table 1 shows the experimental and deterministic aerodynamic forces, C_L and C_D. Tables 2 and 3 indicate that there are no important differences between IPCM and NIPCM in mean, except for NIPCM C_D in the case of Mach number uncertainty. Note that the IPCM results for averaged C_L and C_D are in general closer to the deterministic values than the NIPCM results. The variances of C_L obtained with NIPCM are systematically higher than those of IPCM, whereas the reverse is true for the variances of C_D.

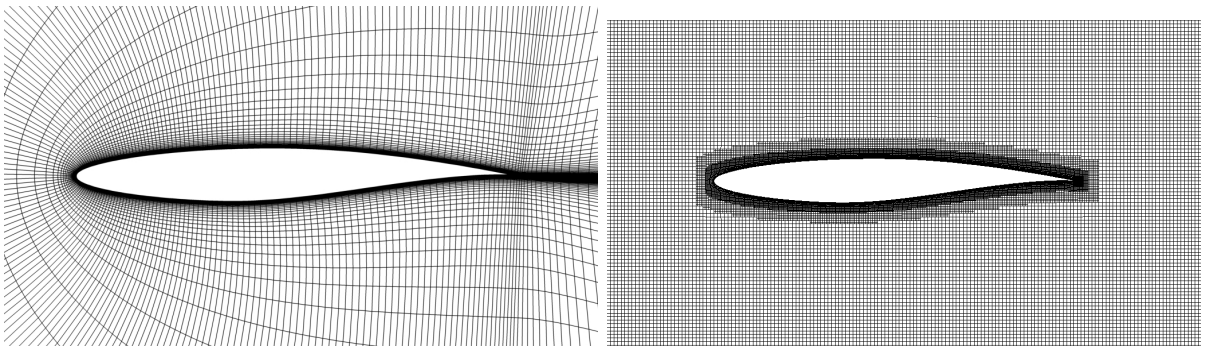

(a) (b)

Figure 1: Grid mesh, (a): FINE^{TM}/ Turbo, (b): FINE^{TM}/ Hexa

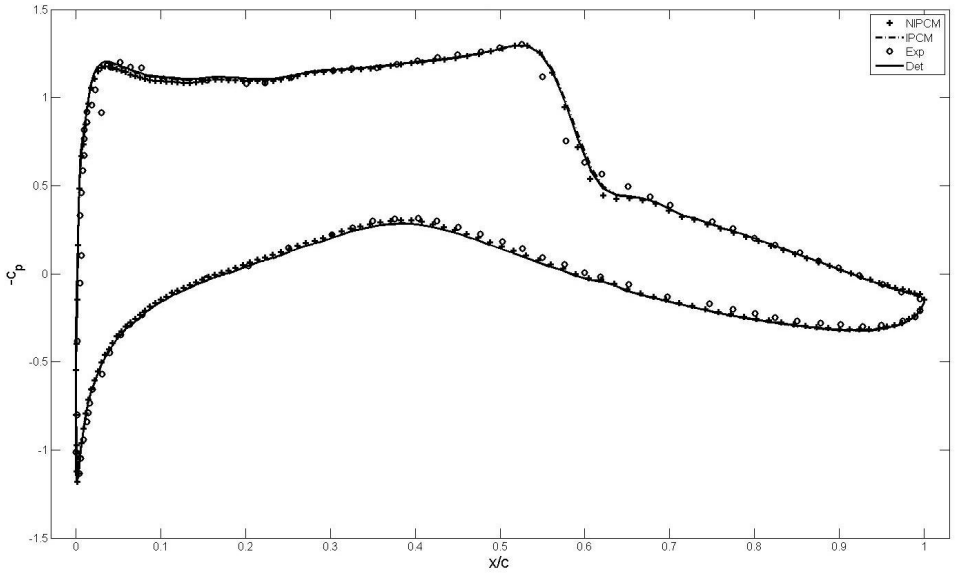

(a)

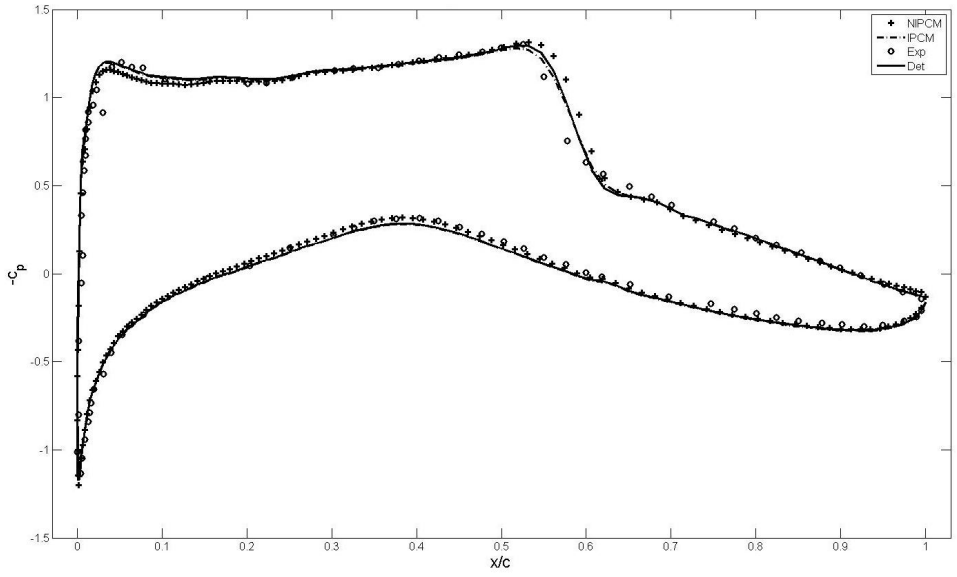

(b)

Figure 2: C_P comparison IPCM vs NIPCM, (a): AOA uncertainty, (b): Mach number uncertainty

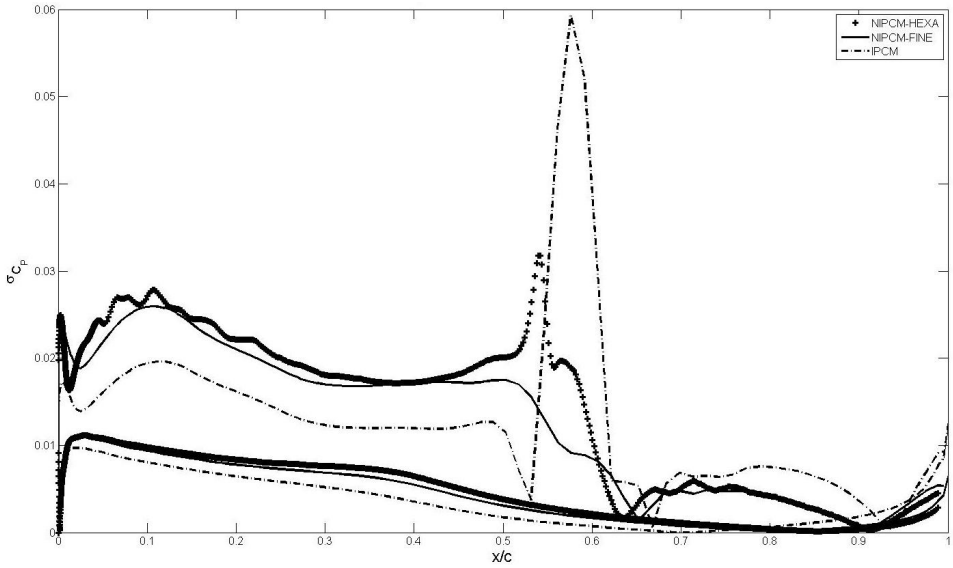

(a)

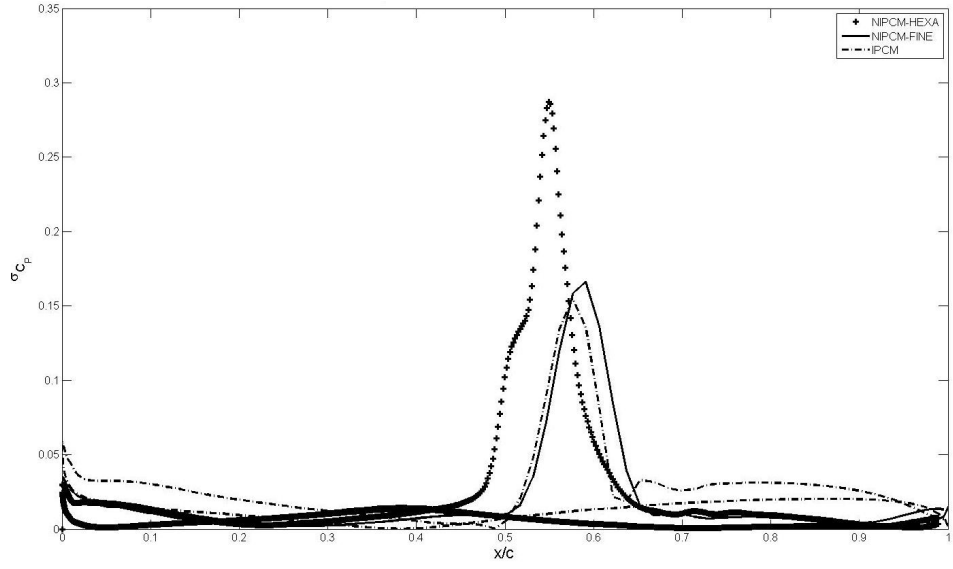

(b)

Figure 3: σ_{C_P} comparison IPCM vs NIPCM, (a): AOA uncertainty, (b): Mach number uncertainty

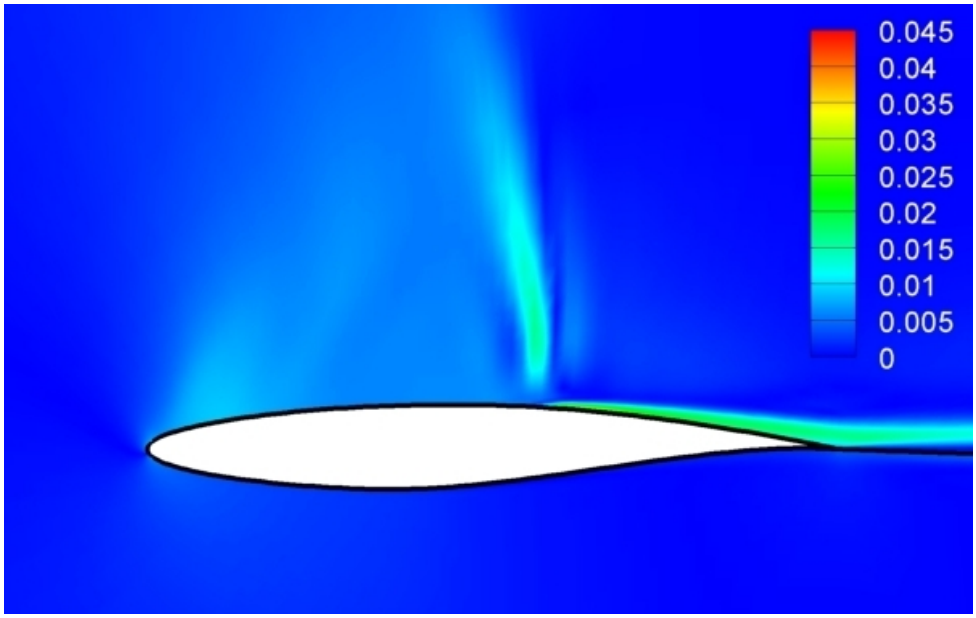

(a)

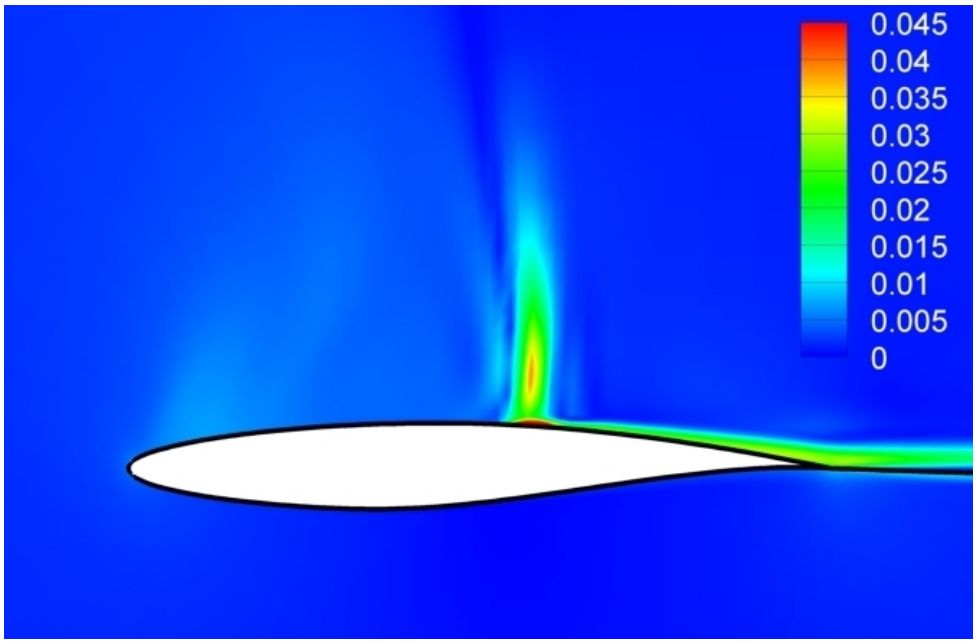

(b)

Figure 4: σ_M AOA uncertainty, (a): Non - intrusive, (b): Intrusive

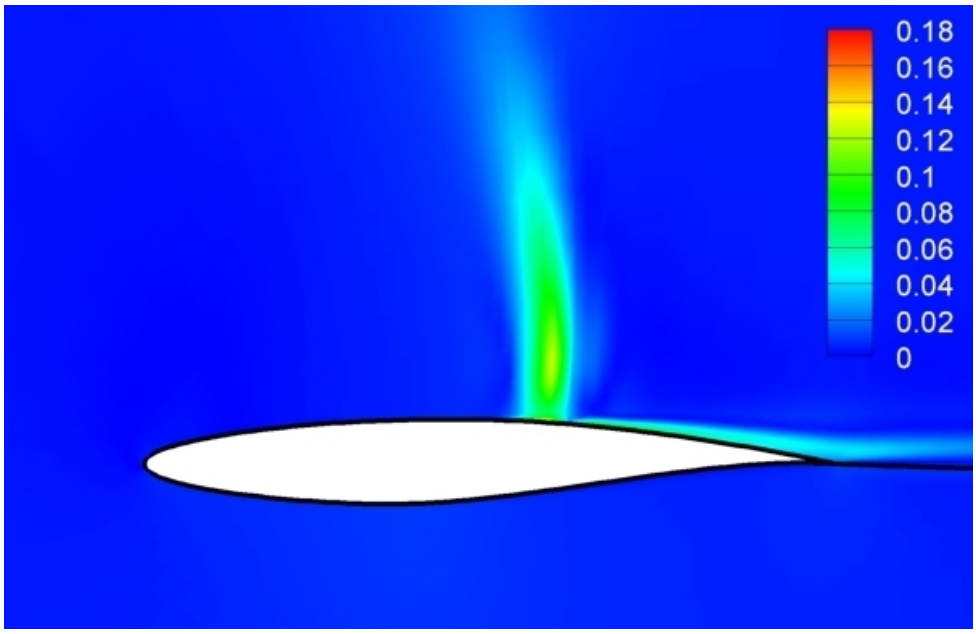

(a)

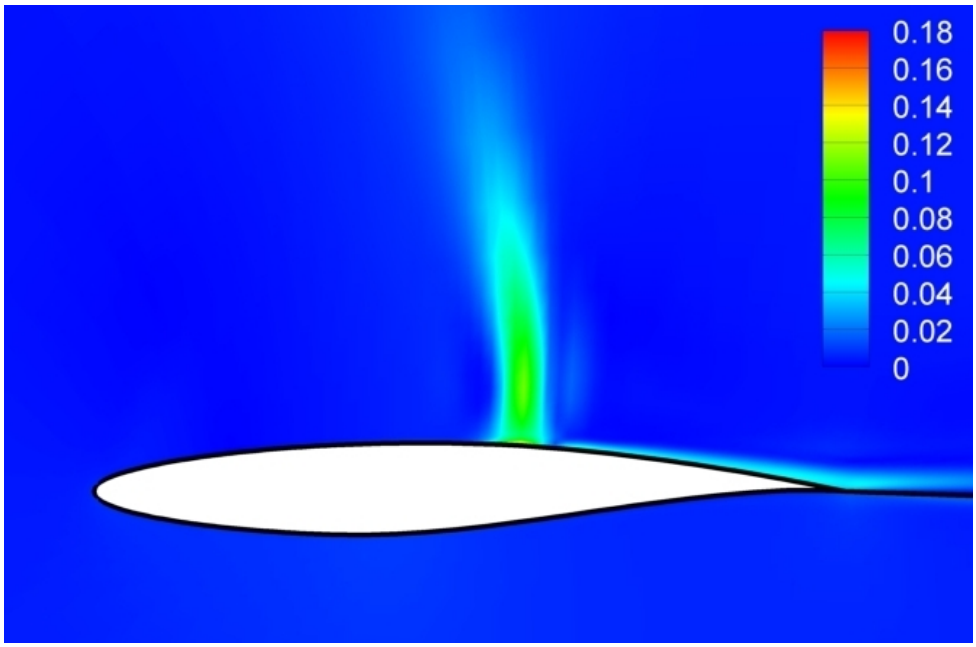

(b)

Figure 5: σ_M Mach number uncertainty, (a): Non - intrusive, (b): Intrusive

C_L		C_D	
$FINE^{TM}/Turbo$	Exp	$FINE^{TM}/Turbo$	Exp
0.84229	0.803	0.01745	0.0168

Table 1: Deterministic and experimental C_L and C_D

C_L		C_D	
$IPCM$	$NIPCM$	$IPCM$	$NIPCM$
0.8427	0.8219	0.01784	0.01751
σ_L		σ_D	
$IPCM$	$NIPCM$	$IPCM$	$NIPCM$
0.00185	0.00849	0.00308	0.00109

Table 2: AOA uncertainty: values computed by IPCM and NIPCM

C_L		C_D	
$IPCM$	$NIPCM$	$IPCM$	$NIPCM$
0.8413	0.8275	0.01764	0.02003
σ_L		σ_D	
$IPCM$	$NIPCM$	$IPCM$	$NIPCM$
0.00469	0.01414	0.00083	0.00032

Table 3: Mach number uncertainty: values computed by IPCM and NIPCM

4 CONCLUSIONS

Results with IPCM and NIPCM for the transonic RAE2822 airfoil have been obtained on identical grids using the same solver. The averaged surface pressure coefficients are quite similar for IPCM and NIPCM, although some deviations are observed especially in the shock region and near leading edge on suction side. In case of uncertain AOA, the variance of C_P along the airfoil does not show a peak near the shock for NIPCM, this in contrast to IPCM. However a NIPCM simulation on a finer grid (with another solver) reveals again this peak, be it smaller than that of IPCM. The same behavior is observed for the variance of Mach number: although no peak can be observed close to the airfoil, there is a substantial increase in the shock region further away from the airfoil. In case of uncertain Mach number, the distributions of variance of C_P along the airfoil are much more similar. The same is true for the variance of Mach number. As for the averaged aerodynamic coefficients (C_L, C_D), these are in general closer to the deterministic values in case of IPCM. The predicted variances of C_L are higher for NIPCM, for both cases (uncertainty on AOA and on Mach), whereas the reverse is true for the variance of C_D.

REFERENCES

[1] C. Dinescu, S. Smirnov, Ch. Hirsch, and C. Lacor. Assessment of intrusive and non - intrusive non - deterministic CFD methodologies based on polynomial chaos expansions. *Int. J. Engineering Systems Modelling and Simulation*, Vol.2, No. 1-2, pp.87-98, 2010.

[2] C. Lacor and S. Smirnov. Uncertainty Propagation in the Solution of Compressible Navier - Stokes Equations using Polynomial Chaos Decomposition. *RTO-MP-AVT-147 Computational Uncertainty in Military Vehicle Design,* 2007. Athens.

[3] G.J.A. Loeven and H. Bijl. Airfoil Analysis with Uncertain Geometry using the Probabilistic Collocation method. *AIAA paper 2008-2070,* 2008. 48$^{\text{th}}$ AIAA/ASME/ASCE/AHS/ASC Structures, Structural Dynamics, and Materials Conference.

[4] G.J.A. Loeven, J.A.S.Witteveen, and H. Bijl. Probabilistic Collocation: An Efficient Non - Intrusive Apporach For Arbitrarily Distributed Parametric Uncertainties. *AIAA paper 2007-317,* 2007. 48$^{\text{th}}$ AIAA/ASME/ASCE/AHS/ASC Structures, Structural Dynamics, and Materials Conference.

[5] N. Wiener. The Homogeneous Chaos.*Am. J. Math.*, 60:897-936, 1938.

[6] R. Askey and J. Wilson. Some Basic Hypergeometrical Polynomials that Generalize Jacobi Polynomials. *Mem. Amer. Math. Soc. 319*, AMS, Providence, RI, 1985.

[7] Ch. Hirsh. Incertitudes dans le domaine des méthodes numériques et méthodes de propagation. 44$^{\text{eme}}$ *Colloque d'Aérodynamique Appliquée*, 23-25 March 2009. Nantes.

[8] G.H. Golub and J.H. Welsch, Calculation of Gauss quadrature rules, *Mathematics of Computation*, Vol. 23, No. 106, 1969, pp. 221230.

[9] W. Gautschi, Orthogonal polynomials (in Matlab), *Journal of Computational and Applied Mathematics*, Vol. 178, 2005, pp. 215234.

[10] M.J. Gander and A.H. Karp, Stable computation of high order Gauss quadrature rules using discretization for measures in radiation transfer, *Journal of Quantitative Spectroscopy Radiative Transfer*, Vol. 68, No. 2, 2001, pp. 213223.

[11] P.H. Cook, M.A. McDonald and M.C.P. Firmin. Aerofoil RAE 2822 - Pressure Distributions, and Boundary Layer and Wake Measurements *Experimental Data Base for Computer Program Assessment*, AGARD Report AR 138, 1979.